A mm-Wave Hybrid Stirring Technique for Over-the-Air Testing in Reverberation Chambers

A mm-Wave Hybrid Stirring Technique for Over-the-Air Testing in Reverberation Chambers

N. Farid[#1], A. Hubrechsen[*#2], J. Fridén[†3], U. Johannsen[#4] A.B. Smolders[*#5], L.A. Bronckers[*#6]

[#]Eindhoven University of Technology, Department of Electrical Engineering, Eindhoven, The Netherlands

[*]Antennex B.V., Eindhoven, The Netherlands

[†]Ericsson Research, Ericsson AB, Gothenburg, Sweden

{[1]s.farid.mohajer, [2]a.hubrechsen, [4]u.johannsen, [5]a.b.smolders, [6]l.a.bronckers }@tue.nl, [3]jonas.friden@ericsson.com

***Abstract*— Over-the-Air methodologies are the potential solutions for the characterization of next-generation wireless devices that rely on the emulation of a realistic channel model in a controlled laboratory environment. A highly attractive concept is the hybrid chamber, combining properties of anechoic chambers and reverberation chambers. By altering the mechanical stirrers of a mm-Wave reverberation chamber, a novel loading condition to achieve a directive channel for 5G NR FR2 applications is proposed: a hybrid stirrer. This is done by partly covering the stirrers with radio-frequency absorbers, as a first step towards a hybrid chamber. In future generations, this may be used to intentionally break uniformity in a controlled manner. Moreover, a more conventional loading configuration is investigated as a counterpart. A spatial uniformity study based on the chamber's power transfer function measurements is carried out for two case scenarios. It has been shown that the proposed configurations are capable of altering spatial uniformity, giving 0.52 dB and 1.46 dB for the conventional and hybrid stirrer method, respectively. Both result in a frequency-flat channel with the required coherence bandwidth for the successful demodulation of the signals.**

***Keywords*— 5G NR FR2, mm-Wave, Reverberation Chamber, RF Loading, Spatial Uniformity, Uncertainty, Wireless Testing**

I. Introduction

The outline for the next generations of communications predicts a migration towards mm-Waves with larger bandwidths. To meet the requirements such as extremely high data rates and ubiquitous coverage as well as low energy consumption and affordable devices, the wireless systems will be designed in an integrated fashion exploiting concepts like Massive Multiple-Input Multiple-Output (mMIMO) and beamforming where the performance of the system would depend on the characteristics of the propagation channel significantly [1]. This gives rise to new challenges in terms of characterization of these systems since the antenna terminals are not accessible to perform conducted tests. Thus, there is a growing demand for measurement setups that are time-efficient, cost-effective, and accurate [2]. Over-the-Air (OTA) methodologies are the potential solution for evaluating the performance of such radio systems in real-life scenarios where a realistic channel model should be emulated in a controlled laboratory environment. This would replace the current time-consuming and hard-to-reproduce drive tests and facilitate the product development procedure and ensure the effective operation and optimal performance of wireless devices under various conditions.

Two common test facilities for performing OTA tests are Anechoic Chambers (AC) and Reverberation Chambers (RC). An anechoic chamber is a room covered by radio absorbing materials to eliminate reflections of electromagnetic waves within and to emulate free-space conditions with a Line-Of-Sight (LOS) link. A reverberation chamber is an electrically large cavity employed with different stirring mechanisms to achieve a rich scattering environment [3]–[5]. In an ideal reverberation chamber the electromagnetic fields are expected to be statistically uniform and isotropic and it mimics a Rich Isotropic MultiPath (RIMP) environment [6]. Given that mm-Wave propagation channels are directional sparse multipath channels [7] and mm-Wave applications cover a wide range of use cases [8]–[12], the aforementioned facilities fall short in terms of channel emulation capabilities and adapting to distinct scenarios. To address this issue, attempts are done to develop a hybrid chamber that exhibits characteristics of both AC and RC. A reverberation chamber is chosen as the starting point in these studies, and is selectively loaded with RF absorbers to emulate a directional channel within [13]–[15]. Nevertheless, the full control of temporal and angular characteristics of the channel is not accomplished yet.

To gain more control over the directionality of the emulated channel, the spatial uniformity of the conventional reverberation chamber should be broken down in a controlled manner. In contrast to the previously proposed hybrid chambers that which large blocks of RF absorbers are used to load the chamber [13]–[15], two novel loading configurations are investigated for this aim. In the first configuration, the RF absorbers are placed on the stirrers to achieve a tuneable, half-absorbing structure instead of the commonly used fully-reflective ones. For the second, more conventional configuration, the same absorbers are placed on the inner walls of the RC strategically. This configuration aims for a more conventional RC performance than the first configuration, which can be considered as a first step towards the realization of spatial channel emulation platforms and adaptive hybrid chambers which would allow conducting the required tests within only one chamber. Both configurations are evaluated and compared in terms of spatial uniformity and coherence bandwidth (CBW), metrics that assess the directional dependencies of the emulated channel and its

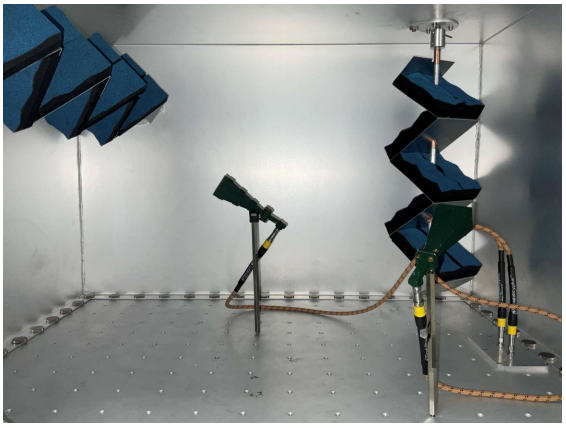

Fig. 1. Chamber configuration A showing placement of the RF absorbers on the stirrers, transmit antenna (oriented toward the vertical stirrer) and receive antenna (oriented towards the horizontal stirrer).

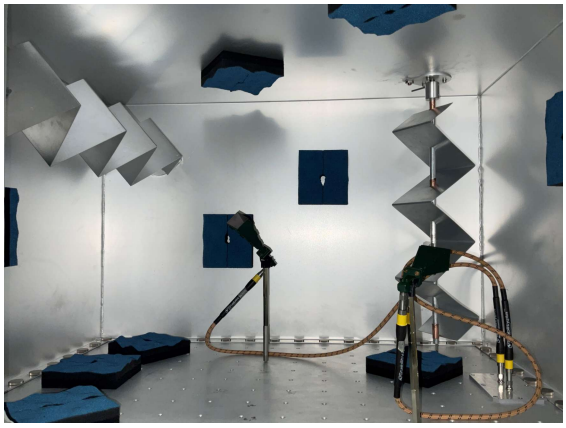

Fig. 2. Chamber configuration B showing placement of the RF absorbers on the walls, transmit antenna (oriented toward the vertical stirrer) and receive antenna (oriented towards the horizontal stirrer).

applicability to demodulation of communication signals. In Section II, the chamber configurations and loading scenarios are demonstrated and the measurement procedure is described. Section III is dedicated to the evaluation of spatial uniformity of each configuration based on the measured power transfer function. Furthermore, the CBW calculations are presented. The conclusion is given in Section IV.

II. Loading Configuration and Measurement Setup

All measurements were performed in a mm-Wave reverberation chamber. The chamber's size is 0.8 m $\times$ 0.6 m $\times$ 0.5 m and it is equipped with two Z-fold stirrers [16]. As shown in Fig. 1, for the first configuration (Config. A) the mechanical stirrers are partly covered with RF absorbers to establish a half-absorbing, half-reflecting stirrer. In this case, a complimentary stirrer is realized after a 180° rotation, i.e. the absorbing plates are replaced by metallic plates and vice versa, following the concept of a hybrid chamber. In the second, more conventional, configuration (Config. B), the same absorbers are spread on the inner surfaces of the RC (Fig. 2). The absorbers are multilayered and carbon-loaded sheet material where the front surface of the material has a shallow convoluted shape.

To quantify the degradation in the spatial uniformity due to the loading of the RC, the method described in [17] was used. For each loading configuration nine measurements were carried out by relocating the transmit antenna within the working volume of the RC. Two WR28 standard gain horn antennas with the gain of 20 dBi were connected to the VNA to measure the S-parameters. The calibration was done using a 2.92mm calibration kit and the reference planes were located at the antenna ports. The antennas were oriented away from each other to minimize the direct coupling. Moreover, the antennas were positioned more than half a wavelength away from the metallic surfaces and the absorbers which at the targeted frequencies correspond to a few millimeters [17]. Care was taken when orienting the antennas to avoid the proximity effect [18]. The stirrers were rotated one at a time with a 36° step, resulting in $N = 100$ mode-stirring samples for each measurement. Using Pearson's correlation and a threshold of 0.3, the independence of each realization was verified. The measurement parameters are summarized in Table 1.

Table 1. Measurement Parameters

Parameter	**Value**
Frequency range	26 GHz - 30 GHz
Number of frequency points	1000 points/GHz
IF bandwidth	1 KHz
VNA output power level	0 dBm
Dwell time	10 μs
Paddles step size (V, H)	36° $\times$ 36°
Number of mode-stirring samples	$10 \times 10 = 100$

The spatial uniformity of each loading configuration is assessed in terms of the chamber power transfer function as follows [19]:

$$G_{\text{ref}} = \frac{\langle |S_{21}|^2 \rangle}{\eta_{\text{TX}} \eta_{\text{RX}} (1 - |\langle S_{11} \rangle|^2)(1 - |\langle S_{22} \rangle|^2)}, \tag{1}$$

where $\langle \cdot \rangle$ denotes the ensemble average over the entire mode-stirring sequence, S_{21} is the measured transmission coefficient, η_{TX} and η_{RX} are antenna radiation efficiencies, and S_{11} and S_{22} are reflection coefficients to correct for antenna mismatches. G_{ref} was calculated for nine independent locations within the working volume of the chamber for each configuration. The uniformity is quantified by the standard deviation between the different positions and is given by [17]:

$$\sigma_{G_{\text{ref}}} = \sqrt{\frac{1}{P-1} \sum_{p=1}^{P} \left(G_{\text{ref},p} - \widehat{G}_{\text{ref}} \right)^2}, \tag{2}$$

where $P = 9$ is the number of the measured positions, i.e. location and orientation, p is the position number, $G_{\text{ref},p}$ is the chamber transfer function for the position p, and $\widehat{G}_{\text{ref}}$ is the transfer function averaged over all stirring sequence. Using the following equation, G_{ref} can be expressed in dB scale:

$$\sigma_{G_{\text{ref,dB}}} = 10 \log_{10} \left(\frac{\widehat{G}_{\text{ref}} + \sigma_{G_{\text{ref}}}}{\widehat{G}_{\text{ref}}} \right). \tag{3}$$

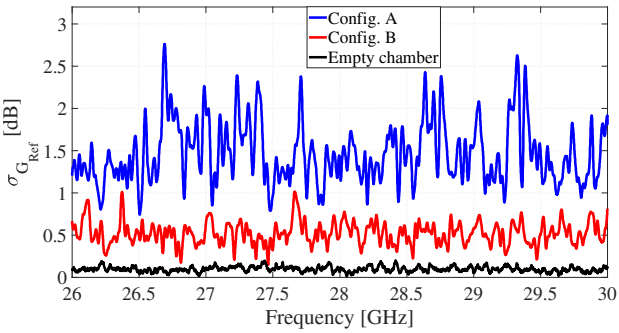

Fig. 3. Standard deviation in G_{ref} over frequency between nine antenna locations.

Placing RF absorbers in the chamber introduces additional losses, hence, the quality factor is reduced and the CBW is broadened compared to an empty chamber. Similar to the definition in propagation channels, the CBW indicates the minimum frequency difference between uncorrelated signals [19]. The CBW wider than the channel's bandwidth is crucial for distortionless demodulation of the signals. For 5G NR FR2 the maximum channel bandwidths of 50/100/200/400 MHz is specified in [20]. The CBW is computed from the frequency autocorrelation of an S_{21} measurement for a given threshold as [17]:

$$R(\Delta f_i, n_i) = \frac{\sum_{j=1}^{M} S_{21}(f_j, n_i) S_{21}^*(f_j + \Delta f_i, n_i)}{\sum_{j=1}^{M} S_{21}(f_j, n_i) S_{21}^*(f_j, n_i)}, \quad (4)$$

where $S_{21}(f_j, n_i)$ is the measured complex S_{21} at frequency step f_j with M frequency points measured within the bandwidth of interest, Δf_i corresponds to one of several frequency offsets over the bandwidth of interest, the index n_i is the mode-stirring sample (out of N), and the asterisk denotes complex conjugation.

III. Measurement Results and Discussion

The standard deviation in G_{ref} between the nine antenna locations for the proposed configurations is computed according to (2) and the results are shown in Fig. 3. As reflected in Fig. 3, both configurations deteriorate the uniformity compared to the unloaded case, which has an averaged standard deviation of only 0.09 dB [16]. In the case of a hybrid chamber, this may be a desired effect. The estimated average standard deviation in G_{ref} measurements for the Config. A and Config. B are 1.46 dB and 0.52 dB, respectively. The higher standard deviation in G_{ref} of Config. A might be due to the fact that covering stirrers with absorbers reduces their stirring efficiency, hence, nonuniform electromagnetic fields are achieved. The uncertainty introduced by the lack of spatial uniformity for the Config. A and Config. B are 0.5 dB and 0.1 dB, respectively, which are within the agreed range of ±1.5 dB in the 3GPP NR standard [21].

Loading the reverberation chamber with RF absorbers flattens the channel's frequency response. Therefore, the required coherence bandwidth for OTA tests is achieved.

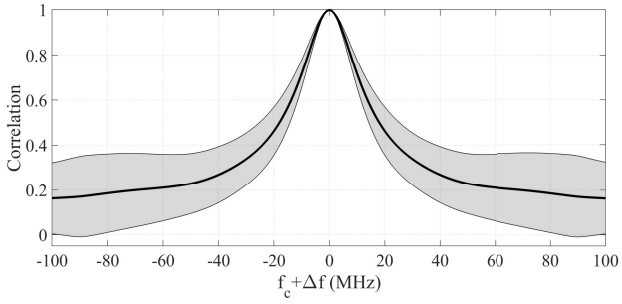

Fig. 4. Best-estimate of coherence bandwidth for Config. A.

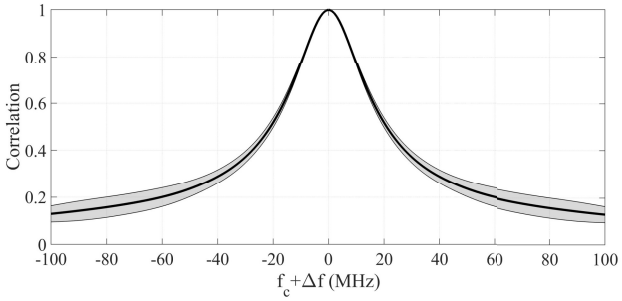

Fig. 5. Best-estimate of coherence bandwidth for Config. B.

The best-estimate coherence bandwidths for both loading configurations are extracted from the average of nine positions and they are shown in Fig. 4 and Fig. 5 where the shaded area represents the deviation among these positions computed as mean-value of CBW$\pm$2std$_{\text{CBW}}$. Despite the use of the same absorbers, the exposed surfaces of the absorbers in the two configurations differ from each other. Consequently, they are distinguishable in terms of how effectively they load the RC. The estimated CBW of Config. A with 0.5 threshold is 36 MHz, while for the Config. B the CBW is 41 MHz. The calculated CBW for the Config. B is similar to the reported CBW of 40 MHz at 45 GHz where an RC with inner dimensions of 1 m $\times$ 0.65 m $\times$ 0.55 m was loaded with six absorbing blocks [22]. Comparing Fig. 4 and Fig. 5, Config. A exhibits higher variation on the CBW. The reason behind this phenomenon may be two fold: first, higher measurement uncertainty in Config. A is translated into higher variation in CBW, second, not only does the number of absorbers have a significant influence on the characteristics of the emulated channel but also the arrangement of the absorbers is of importance [23]–[25].

IV. Conclusion

Spatial uniformity is of great importance for an ideal reverberation chamber. However, for a hybrid chamber to perform OTA tests with realistic channel conditions, one needs to break down the uniformity in a controlled manner to emulate a spatial channel. In this paper, the spatial uniformity of two different loading configurations was investigated. In the first configuration, the stirrers of the reverberation chamber

were altered by placing absorbers on them. A half-absorbing half-reflecting stirrer varies the angle of reflecting waves disparately, which could be used for a hybrid chamber. For the counterpart configuration, the same absorbers were placed on the inner walls of the RC in a more conventional manner. It has been shown that the proposed hybrid stirring technique significantly alters the uniformity, which is a desired characteristic for the hybrid chamber. The averaged standard deviation in G_{ref} measurements for the first and second loading configuration is 1.46 dB and 0.52 dB, respectively. Future work will include characterizing the power-angle profile of these spatially nonuniform environments. To be able to perform OTA measurements the CBW of the chamber must be broader than channel's bandwidth. The best-estimate of CBW for the first and second configurations is 36 MHz and 41 MHz with a 0.5 threshold, respectively which satisfies the requirements of 5G NR FR2 applications.

ACKNOWLEDGMENT

The authors would like to thank Ad Reniers and Noah Reniers from AntenneX for usage of the automation software. This project has received funding from the European Union's Horizon 2020 research and innovation programme under the Marie Skłodowska-Curie grant agreement No 860023.

REFERENCES

[1] J. G. Andrews, S. Buzzi, W. Choi, S. V. Hanly, A. Lozano, A. C. K. Soong, and J. C. Zhang, "What will 5G be?" *IEEE Journal on Selected Areas in Communications*, vol. 32, no. 6, pp. 1065–1082, 2014.

[2] Y. Qi, G. Yang, L. Liu, J. Fan, A. Orlandi, H. Kong, W. Yu, and Z. Yang, "5G Over-the-Air Measurement Challenges: Overview," *IEEE Transactions on Electromagnetic Compatibility*, vol. 59, no. 6, pp. 1661–1670, 2017.

[3] D. A. Hill, *Electromagnetic Fields in Cavities: Deterministic and Statistical Theories*. IEEE, 2009.

[4] R. Serra, A. C. Marvin, F. Moglie, V. M. Primiani, A. Cozza, L. R. Arnaut, Y. Huang, M. O. Hatfield, M. Klingler, and F. Leferink, "Reverberation chambers a la carte: An overview of the different mode-stirring techniques," *IEEE Electromagnetic Compatibility Magazine*, vol. 6, no. 1, pp. 63–78, 2017.

[5] A. Hubrechsen, K. A. Remley, and S. Catteau, "Reverberation Chamber Metrology for Wireless Internet of Things Devices: Flexibility in Form Factor, Rigor in Test," *IEEE Microwave Magazine*, vol. 23, no. 2, pp. 75–85, 2022.

[6] P.-S. Kildal and J. Carlsson, "New approach to ota testing: Rimp and pure-los reference environments a hypothesis," in *2013 7th European Conference on Antennas and Propagation (EuCAP)*, 2013, pp. 315–318.

[7] T. S. Rappaport, G. R. MacCartney, M. K. Samimi, and S. Sun, "Wideband Millimeter-Wave Propagation Measurements and Channel Models for Future Wireless Communication System Design," *IEEE Transactions on Communications*, vol. 63, no. 9, pp. 3029–3056, 2015.

[8] J. Huang, Y. Liu, C.-X. Wang, J. Sun, and H. Xiao, "5G Millimeter Wave Channel Sounders, Measurements, and Models: Recent Developments and Future Challenges," *IEEE Communications Magazine*, vol. 57, no. 1, pp. 138–145, 2019.

[9] TSGR, "5G; Study on channel model for frequencies from 0.5 to 100 GHz," 3rd Generation Partnership Project (3GPP), Technical Report (TR) 36.331, 2020, version 16.1.0 Release 16.

[10] C. Cano, G. H. Sim, A. Asadi, and X. Vilajosana, "A Channel Measurement Campaign for mmWave Communication in Industrial Settings," *IEEE Transactions on Wireless Communications*, vol. 20, no. 1, pp. 299–315, 2021.

[11] F. Jameel, S. Wyne, S. J. Nawaz, and Z. Chang, "Propagation Channels for mmWave Vehicular Communications: State-of-the-art and Future Research Directions," *IEEE Wireless Communications*, vol. 26, no. 1, pp. 144–150, 2019.

[12] D. He, K. Guan, J. M. García-Loygorri, B. Ai, X. Wang, C. Zheng, C. Briso-Rodríguez, and Z. Zhong, "Channel Characterization and Hybrid Modeling for Millimeter-Wave Communications in Metro Train," *IEEE Transactions on Vehicular Technology*, vol. 69, no. 11, pp. 12 408–12 417, 2020.

[13] M. Becker, R. Horansky, D. Senic, V. Neylon, and K. Remley, "Spatial Channels for Wireless Over-the-Air Measurements in Reverberation Chambers," vol. 2018. Institution of Engineering and Technology, pp. 495 (5 pp.)–495 (5 pp.).

[14] J. Kvarnstrand, P. Svedjenäs, E. Silfverswärd, and H. Helmius, "Integrating LoS and RIMP Measurements in a Single Test Environment," in *2021 15th European Conference on Antennas and Propagation (EuCAP)*, 2021, pp. 1–5.

[15] A. Sorrentino, F. Nunziata, S. Cappa, S. Gargiulo, and M. Migliaccio, "A Semi-Reverberation Chamber Configuration to Emulate Second-Order Descriptors of Real-Life Indoor Wireless Propagation Channels," *IEEE Transactions on Electromagnetic Compatibility*, vol. 63, no. 1, pp. 3–10, 2021.

[16] A. Hubrechsen, A. C. F. Reniers, A. B. Smolders, and L. A. Bronckers, "Chamber-Decay Time in a mm-Wave Reverberation Chamber," in *2021 IEEE International Symposium on Antennas and Propagation and USNC-URSI Radio Science Meeting (APS/URSI)*, 2021, pp. 835–836.

[17] "Test Plan for Wireless Large-Form-Factor Device Over-the-Air Performance," 2019. [Online]. Available: www.ctia.org/certification

[18] W. T. C. Burger, C. L. Holloway, and K. A. Remley, "Proximity and orientation influence on Q-factor with respect to large-form-factor loads in a reverberation chamber," in *2013 International Symposium on Electromagnetic Compatibility*, 2013, pp. 369–374.

[19] K. A. Remley, J. Dortmans, C. Weldon, R. D. Horansky, T. B. Meurs, C.-M. Wang, D. F. Williams, C. L. Holloway, and P. F. Wilson, "Configuring and Verifying Reverberation Chambers for Testing Cellular Wireless Devices," *IEEE Transactions on Electromagnetic Compatibility*, vol. 58, no. 3, pp. 661–672, 2016.

[20] ETSI, "5G; NR; User Equipment (UE) radio transmission and reception; Part 1: Range 1 Standalone," 3rd Generation Partnership Project (3GPP), Technical Report (TR) 38.101-1, 09 2021, version 15.14.0.

[21] 3GPP, "Radio Frequency (RF) conformance testing background for radiated Base Station (BS) requirements," 3rd Generation Partnership Project (3GPP), Technical Report (TR) 37.941, 09 2021, version 16.3.0.

[22] D. Senic, K. A. Remley, M. G. Becker, and C. L. Holloway, "Spatial Uniformity Study in a Loaded Reverberation Chamber at Millimeter-Wave Frequencies," in *2018 IEEE Symposium on Electromagnetic Compatibility, Signal Integrity and Power Integrity (EMC, SI PI)*, 2018, pp. 467–472.

[23] L. Bastianelli, L. Giacometti, V. M. Primiani, and F. Moglie, "Effect of absorber number and positioning on the power delay profile of a reverberation chamber," in *2015 IEEE International Symposium on Electromagnetic Compatibility (EMC)*, 2015, pp. 422–427.

[24] A. Sorrentino, G. Ferrara, and M. Migliaccio, "The Reverberating Chamber as a Line-of-Sight Wireless Channel Emulator," *IEEE Transactions on Antennas and Propagation*, vol. 56, no. 6, pp. 1825–1830, 2008.

[25] J. B. Coder, J. M. Ladbury, C. L. Holloway, and K. A. Remley, "Examining the true effectiveness of loading a reverberation chamber: How to get your chamber consistently loaded," in *2010 IEEE International Symposium on Electromagnetic Compatibility*, 2010, pp. 530–535.